

α -clustering effects in dissipative $^{12}\text{C} + ^{12}\text{C}$ reactions at 95 MeV

G. Baiocco,^{1,2,*} L. Morelli,¹ F. Gulminelli,² M. D'Agostino,¹ M. Bruno,¹ U. Abbondando,³ S. Barlini,^{4,5} M. Bini,^{4,5} S. Carboni,^{4,5} G. Casini,⁵ M. Cinausero,⁶ M. Degerlier,⁷ F. Gramegna,⁶ V. L. Kravchuk,^{6,8} T. Marchi,^{6,9} A. Olmi,⁵ G. Pasquali,^{4,5} S. Piantelli,⁵ and Ad. R. Raduta¹⁰

¹*Dipartimento di Fisica e Astronomia dell'Università di Bologna and INFN, Bologna, Italy*

²*LPC (IN2P3-CNRS/Ensaclen et Université), F-14076 Caen cedex, France*

³*INFN Trieste, Italy*

⁴*Dipartimento di Fisica e Astronomia dell'Università, Firenze, Italy*

⁵*INFN Firenze, Italy*

⁶*INFN, Laboratori Nazionali di Legnaro, Italy*

⁷*University of Nevsehir, Science and Art Faculty, Physics Department, Nevsehir, Turkey*

⁸*National Research Center "Kurchatov Institute," Moscow, Russia*

⁹*Dipartimento di Fisica e Astronomia dell'Università degli Studi di Padova, Padova, Italy*

¹⁰*NIPNE, P.O. Box MG-6, Bucharest-Magurele, Romania*

(Received 30 January 2013; published 22 May 2013)

Dissipative $^{12}\text{C} + ^{12}\text{C}$ reactions at 95 MeV are fully detected in charge with the GARFIELD and RCo apparatuses at Laboratori Nazionali di Legnaro. A comparison to a dedicated Hauser-Feshbach calculation allows us to select events which correspond, to a large extent, to the statistical evaporation of highly excited ^{24}Mg , as well as to extract information on the isotopic distribution of the evaporation residues in coincidence with their complete evaporation chain. Residual deviations from statistical behavior are observed in α yields and attributed to the persistence of cluster correlations well above the ^{24}Mg threshold for six- α decay.

DOI: [10.1103/PhysRevC.87.054614](https://doi.org/10.1103/PhysRevC.87.054614)

PACS number(s): 25.70.-z, 24.60.Dr, 27.30.+t, 24.10.Pa

I. INTRODUCTION

Since the first heuristic proposition of α chains as possible building blocks of even-even nuclei in the late 1960s [1], the subject of α clustering has been a central issue in nuclear physics and even witnessed a gain of interest in recent years [2]. On the theoretical side, *ab initio* calculations have shown cluster features in the ground state of a large number of light nuclei [3] as well as in some excited states around the threshold energy of breakup into constituent clusters, showing that cluster correlations are indeed a ubiquitous feature of quantum few-body systems down to the femtometer scale. In experimental research, rotational bands consistent with α -cluster structures have been identified in different even-even light nuclei and shown to persist even along their isotopic chains [2]. Exotic nonstatistical decays of these correlated states have been evidenced in the recent literature [4].

A natural extension of these correlations concerns nuclear molecules. Molecular states have been sought for since the early days of heavy-ion science. In particular, several interesting resonances have been observed in the $^{12}\text{C} + ^{12}\text{C}$ reaction in the inelastic [5] and α -transfer channels [6]. These studies suggest that resonant structures persist in the ^{24}Mg system up to around 50 MeV excitation energy, a remarkable result as a pure statistical behavior might be expected due to the extremely high number of available states at such high excitation. For the α -transfer channel, experimental results have been reproduced by coupled cluster calculations [7] where the cross section is dominated by a four-cluster ($\alpha + \alpha$) + ($\alpha + ^{12}\text{C}$) state of

highly excited ^{24}Mg around 30 MeV. The question then naturally arises whether such correlations might affect more dissipative channels which are typically associated with the formation of a compound nucleus, that is, a system whose decay is assumed to be fully decoupled from the reaction entrance channel and governed by purely statistical laws.

This effect might be experimentally seen as an excess of cluster production with respect to the prediction of the statistical model, provided that the ingredients of the latter are sufficiently constrained via experimental data. To this aim, we have performed an exclusive and (quasi)complete detection of the different decay products emitted in $^{12}\text{C} + ^{12}\text{C}$ dissipative reactions at 95 MeV and compared experimental data to a dedicated Hauser-Feshbach (HF) code, with transmission coefficients and level densities optimized on the $A \approx 20$ region [8].

In this paper we will show that all the observables of dissipative events are fully compatible with standard statistical behavior, with the exception of α yields in coincidence with oxygen residues. The observed anomalies are tentatively attributed to clustering effects which appear to survive even in the most dissipative events. The plan of the paper is as follows. In the next section the experiment and data selection are briefly presented. The experimental results are systematically compared to Hauser-Feshbach calculations in Sec. III, and the anomalous behavior of the $^{12}\text{C} + ^{12}\text{C} \rightarrow xn + 2\alpha + ^{16-x}\text{O}$ channel is evidenced. Conclusions are drawn in Sec. IV.

II. EXPERIMENT AND DATA SELECTION

The experiment was performed at the Laboratori Nazionali di Legnaro (LNL), with the ^{12}C beam provided by the XTU

*Present address: Dipartimento di Fisica dell'Università di Pavia, Italy; giorgio.baiocco@pv.infn.it

TANDEM accelerator. The experimental setup comprised the GARFIELD detector, made up of two drift chambers, filled with CF_4 gas, azimuthally divided into 24 sectors, each one consisting of 8 ΔE - E telescopes, for a total of 180 telescopes. The residual energy of the reaction products was measured by CsI(Tl) scintillation detectors, with an energy resolution of about 4%. GARFIELD covers the polar angular range from 30° to 150° . Forward laboratory angles in the range $5^\circ \leq \theta \leq 18^\circ$ are covered by the Ring Counter (RCo), which is a three-stage telescope device [ionization chamber (IC), strip silicon detector, and CsI(Tl) scintillator]. The angular resolution of each of the 64 strips is $\pm 0.8^\circ$. The typical energy resolutions of such devices are less than 0.5% full width at half maximum (FWHM) for the silicon strips, 3%–4% FWHM for the CsI crystals, and less than 10% FWHM for the gas detectors. More details can be found in Refs. [9,10]. The combination of the two devices allows a nearly 4π coverage of the solid angle, which, combined with a high granularity, permits measurement of the charge, energy, and emission angles of nearly all charged reaction products, allowing an excellent discrimination of different reaction mechanisms.

Events with a single $Z \geq 2$ fragment detected in the RCo in coincidence with one or more light charged particles (LCPs) $Z \leq 3$ in GARFIELD are selected. LCP isotopic identification has been performed through fast and slow CsI analysis [11], with energy thresholds [12] similar to those of other experimental 4π devices [13].

Only events where the total charge of the entrance channel, $Z_{\text{det}} = 12$, is detected are kept for the analysis, unless specified in the text. We expect that most of the selected events should correspond to fusion-evaporation reactions, with the residue detected at forward angles in coincidence with evaporated particles detected at central center-of-mass angles covered by GARFIELD. Data are therefore compared to the predictions of a Monte Carlo HF code [8] for the evaporation of the compound nucleus ^{24}Mg , at $E_{\text{fus}}^* = 61.4$ MeV, corresponding to a complete fusion source, and filtered through a software replica of the setup. The maximum angular momentum for the fused system is assumed from PACE4 [14] to be $J_{0\text{max}} = 12\hbar$. The comparison of experimental observables and code calculations is used to validate the parametrization of statistical model ingredients implemented in the code and to gain insight into the deviations from statistical behavior observed in the decay.

III. DATA ANALYSIS

A. Particle spectra

Figure 1 displays the energy spectra of protons and α 's detected in GARFIELD in coincidence with the most abundant residues. If not explicitly stated, all distributions are shown normalized to a unitary area, and all energies are given in the laboratory frame. Experimental data are always shown with statistical error bars, when visible. A very good reproduction of the proton energy spectra is achieved in all channels, while a large discrepancy in the shape of the distribution appears for α 's in coincidence with oxygen residues.

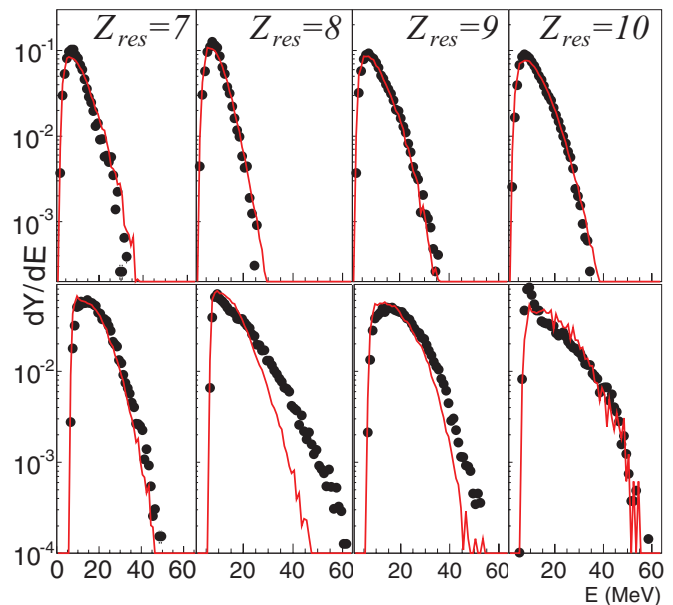


FIG. 1. (Color online) Proton (upper part) and α (lower part) energy spectra in complete $Z_{\text{det}} = 12$ events detected in coincidence with a residue of charge Z_{res} , indicated in each figure column. Data (dots) are compared to model calculations (red lines).

The spectrum shape in a statistical process is determined by the interplay of all physical ingredients entering in the decay, notably transmission coefficients, angular momentum distribution, and level density parameters. Nevertheless, these ingredients can be largely disentangled [15]: transmission coefficients define the shape of evaporated spectra in the Coulomb barrier region; the level density mostly affects the tail slope; and the angular momentum steepens the tail of heavy particles (α 's) with respect to light ones (protons). On the basis of such considerations it is found that no common choice of parameters can be made in our calculations that reproduce at the same time all the measured observables, including α 's in coincidence with an oxygen residue. The best model reproduction is obtained with standard fiducial values [8], as shown in Fig. 1 and will be also shown for other observables below. While proton spectra are very well reproduced whatever the selected channel, the major discrepancy for α 's in the channel where they are accompanied by an oxygen suggests an out-of-equilibrium emission for this specific channel.

B. Direct versus dissipative components

To understand the deviation, a more exclusive channel-by-channel comparison is needed. Figure 2 displays the experimental (left panel) and theoretical (right) correlation between the oxygen energy E_{res} and the sum of the energies of the two α 's, $E\alpha_i$, in $^{12}\text{C}(^{12}\text{C}, ^A\text{O})\alpha\alpha$ events. The lines represent the kinematical locus $Q_{\text{kin}} = E_{\text{res}} + \sum_{i=1,2} E\alpha_i - E_{\text{beam}} = -15.78$ MeV. This locus divides the $(E_{\text{res}}, \sum_{i=1,2} E\alpha_i)$ plane into two regions: in the one above, we find two correlated bands centered, respectively, at $Q_{\text{kin}} = (1.27 \pm 1.40)$ and (-5.35 ± 1.70) MeV, while a broader region extends below the locus up to a high amount of missing energy. In the statistical

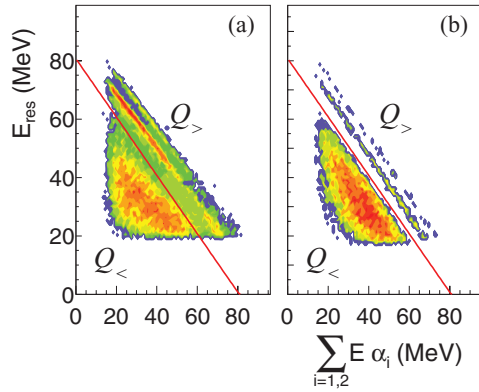


FIG. 2. (Color online) Experimental (a) and theoretical (b) correlation between the energy of the oxygen fragment and the sum of the energies of the two α 's in $^{12}\text{C}(^{12}\text{C},^A\text{O})\alpha\alpha$ events. The red line shows the kinematical locus $Q_{\text{kin}} = E_{\text{res}} + \sum_{i=1,2} E\alpha_i - E_{\text{beam}} = -15.78$ MeV at the opening of the four-body channel $^{12}\text{C}(^{12}\text{C},^{15}\text{O})n\alpha\alpha$ separating dissipative ($Q_{<}$) and nondissipative ($Q_{>}$) events.

model interpretation, the two correlated bands correspond to α -decay chains, starting from the $^{24}\text{Mg}^*$ compound nucleus and leaving an ^{16}O residue either in its ground state ($Q_{\text{kin}} = -0.11$ MeV) or in its excited bound states ($E^* = 6.05, 6.13, 6.92$, or 7.12 MeV), not resolved in the experiment, with a measured average energy expense $Q_{\text{kin}} \approx -6.55$ MeV. Due to the finite energy and angular resolutions and to the energy thresholds the two loci are broadened, remaining compatible with the expected values within the quoted widths. The locus $Q_{\text{kin}} = -15.78$ MeV gives the threshold Q value where the four-body channel $^{12}\text{C}(^{12}\text{C},^{15}\text{O})n\alpha\alpha$ opens. In terms of energy, this is the less expensive channel involving an oxygen residue and particles other than α 's. Neutrons are not detected in this experiment, and the broader distribution observed for lower Q_{kin} values is due to events in which neutron emission has taken place. According to model calculations, the $(n, 2\alpha, ^{15}\text{O})$ channel should absorb the largest cross section in this region. In the following, we will refer to these regions as, respectively, the nondissipative and dissipative events region, and we will adopt for them the notation $Q_{>}$ and $Q_{<}$.

A similar pattern is observed between experimental data and calculations in Fig. 2 for the $(2\alpha, ^A\text{O})$ energy correlation. However, a difference in the relative population of the Q_{\leq} regions is evident: a much higher percentage ($37 \pm 5\%$) of $(2\alpha, ^A\text{O})$ events populates the $Q_{>}$ region in the experimental sample, with respect to $(9 \pm 1\%)$ according to model predictions.¹ Events falling in the $Q_{>}$ region correspond to low-energy dissipation. Therefore, this region can also be populated by reactions not proceeding through an intermediate compound nucleus state. The larger experimental branching ratio for the $(2\alpha, ^{16}\text{O})$ exit channel in the $Q_{>}$ region probably reflects a contamination of direct (α -transfer and pick-up) reactions, in competition with fusion-evaporation reactions. Events falling

¹In all the experimental percentages, the associated error takes into account both the statistical error and the possible ^3He - α contamination.

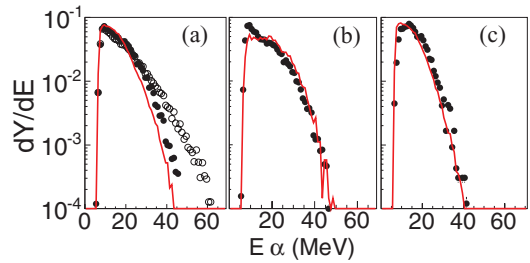


FIG. 3. (Color online) For dissipative events (as defined in the text) with $Z_{\text{det}} = 12$, experimental (black dots) and calculated (red lines) α energy spectra in coincidence with an oxygen are compared for all channels involving at least one α (a) and, separately, channels involving two α 's (b) and only one α (c). As a reference, in the leftmost panel, also the α energy distribution without any Q_{kin} selection (same as in Fig. 1) is shown (empty dots).

in the highly dissipative $Q_{<}$ region, where the contamination of direct reactions can be excluded, are hereafter scrutinized, by looking for deviations from the statistical predictions that can be ascribed to cluster correlations associated with the $^{12}\text{C} + ^{12}\text{C}$ system persisting up to high center-of-mass energies.

Figure 3(a) displays the comparison between data and calculations for the energy spectrum of α particles detected in coincidence with an oxygen residue and emitted in dissipative events (full dots). The α energy distribution without any Q_{kin} selection (empty dots; see Fig. 1) is also plotted. A great improvement in the agreement between data and calculation is achieved when we limit the comparison to the $Q_{<}$ event class. Nevertheless, a residual discrepancy is observed, and the experimental distribution is still not reproduced in its shape. To investigate the origin of this deviation, in Figs. 3(b) and 3(c) we show the α energy distributions associated with channels where the oxygen residue is in coincidence with, respectively, two α 's or only one α . We can see that the shape of the energy spectra depends on the channel. The statistical calculation is able to satisfactorily reproduce separately the energy distributions of particles for dissipative two- α and one- α completely reconstructed decay chains, while the sum of the two processes is not correctly reproduced. This can be understood by considering that, for a completely defined channel and a selected Q value interval, and under the constraint of energy conservation, the shape of the particle spectrum is entirely defined by the kinematics and therefore reproduced by any modelization respecting the kinematical constraints. The discrepancy in the total spectrum is also small, because of the great importance of kinematical correlations in such precisely selected channels. However, a residual difference can be seen. This difference originates from a very important discrepancy in the branching ratios toward the different channels. Experimentally, $(63 \pm 5\%)$ of the total cross section for completely reconstructed dissipative decays with an α particle and an oxygen fragment in the outgoing channel is absorbed by $(2\alpha, ^{16}\text{O}^*)$ channels, where the oxygen is excited above its neutron emission threshold, while according to the theoretical predictions these channels should represent only $(10 \pm 1\%)$ of this class of events. The

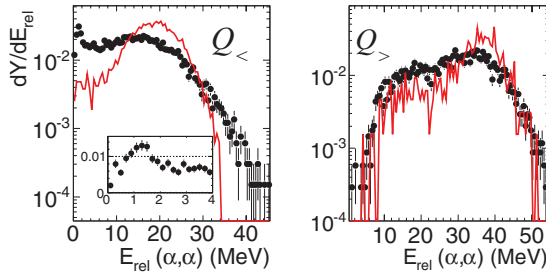


FIG. 4. (Color online) Experimental (black dots) and calculated (red lines) relative energy distributions of the two α 's in coincidence with an oxygen in dissipative (left) and nondissipative (right) events. In the left panel, an enlargement of the low relative energy region with a reduced energy binning is shown in the figure inset, to better reveal the structures of the energy correlation.

residual deviation observed in Fig. 3(a) thus comes from a branching ratio discrepancy for the $(n, 2\alpha, {}^{15}\text{O})$ [and, with a minor contribution, for the $(2n, 2\alpha, {}^{14}\text{O})$] decay channel with respect to decay channels involving a single α emission, even if a contribution from high-energy γ emission from collective states cannot be *a priori* excluded.

This finding indicates that cluster correlations associated with the ${}^{12}\text{C} + {}^{12}\text{C}$ system persist up to higher center-of-mass energies than previously expected from the analysis of the inelastic channel [5] and lead to a nonstatistical behavior in the decay of the highly excited ${}^{24}\text{Mg}$. Given the high excitation energy $E_{\text{fus}}^* = 61.4$ MeV it is not possible to associate the extra yield with a single isolated state with a well-defined angular momentum and parity. Nevertheless, interesting information can be extracted from Fig. 4, which displays the α - α relative energy distribution for the $Q_{<}$ and the $Q_{>}$ regions, in comparison with the statistical model calculation. We can see that a peak appears in the most dissipative events, which can be associated with doorway (${}^8\text{Be}$ - ${}^{16}\text{O}^*$) and (${}^9\text{Be}^*$ - ${}^{15}\text{O}$) states, where the excitation energy of the ${}^{16}\text{O}$ (${}^9\text{Be}$) is above the neutron emission threshold, and which is not present in the statistical model. Due to the limited angular resolution of our experimental device and to the energy thresholds [12] we cannot observe, as in other experimental cases [4] performed at lower beam energies, a well-defined peak corresponding to the decay of ${}^8\text{Be}$ (g.s.). As can be seen in the inset of Fig. 4 the peak at about 1.5 MeV relative energy results indeed from the superposition of the high-energy tail of the ${}^8\text{Be}$ (g.s.) decay with the ${}^9\text{Be}^*$ (1.684 MeV) decay in $n + {}^8\text{Be}$ (g.s.). The contribution of the decay from the broad ${}^8\text{Be}$ level ($E^* = 3.03$ MeV, $\Gamma = 1.6$ MeV) can be guessed at energies above 2 MeV, but higher statistics would be needed to extract quantitative yields. The absence of ${}^8\text{Be}$ resonances in the less dissipative events suggests that these reactions do not originate from an $(\alpha + \alpha) + (\alpha + {}^{12}\text{C})$ doorway state as was suggested to be the case at lower energies [7].

C. Isotopic, charge, and velocity distributions

Since we have interpreted the observed extra α yield as associated with the production of neutron-poor oxygen isotopes, we expect that a signature of the anomalous branching

ratio should be evidenced in the isotopic residue distribution. Unfortunately, the residue mass is not directly accessible in this experiment, because of the low energy of heavier fragments. However, due to the completeness of the detection, this information can be approximately deduced from the calorimetric energy distribution, as explained hereafter.

In each event associated with the production of a residue of mass number A_{res} , the excitation energy is given by the energy balance

$$E_{\text{cal}}^*(A_{\text{res}}) = \sum_i^{N_c} E_i^{CM} + N_n(A_{\text{res}}) \cdot \langle E_n^{CM} \rangle + Q(A_{\text{res}}), \quad (1)$$

where $N_c(N_n)$ and E_i^{CM} ($\langle E_n^{CM} \rangle$) are, respectively, the charged products (neutron) multiplicity and their center-of-mass kinetic energies, and Q is the decay Q value. In a fusion reaction the excitation energy E_{fus}^* is also theoretically known from the entrance channel energy balance. If the neutron energy was measured, Eq. (1) could then be used to deduce the value of A_{res} . In our case, we make the hypothesis that the neutron energy can be (on average) estimated from the measured proton energy with the subtraction of the Coulomb barrier. An estimation of the mass of the residue can thus be obtained by minimizing in each event completely detected in charge the

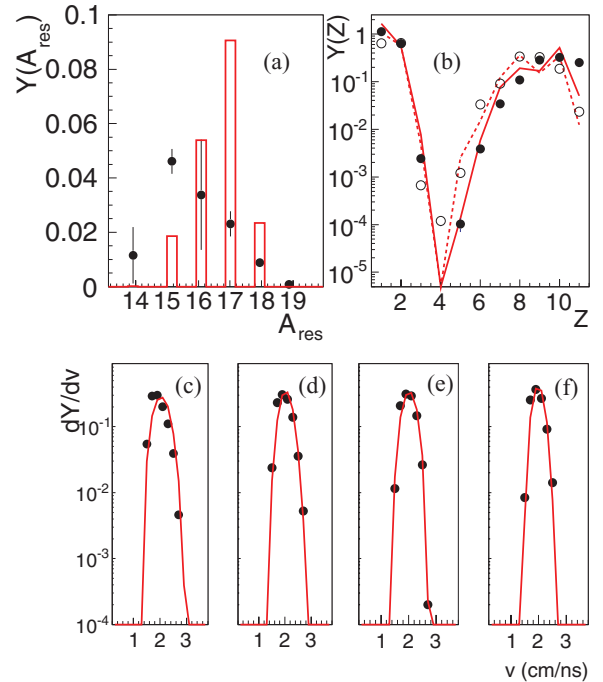


FIG. 5. (Color online) (a) The experimental oxygen isotopic distribution (see text; black dots) compared to the model predictions (red histogram) for all events. (b) Charge distribution, and velocity distributions of the most abundant residues (charge $Z_{\text{res}} = 7, 8, 9, 10$ in panels c, d, e, and f, respectively) are compared for data (dots) and model (lines) after the exclusion of nondissipative events. For the charge distribution, data for complete ($Z_{\text{det}} = 12$, black points) and quasicomplete ($Z_{\text{det}} \geq 10$, empty points) events are compared to model calculations (solid and dashed lines, respectively). Mass and charge distributions are normalized to the number of events retained in the analysis.

quantity $\delta\varepsilon_{\text{cal}}^*(A_{\text{res}}) = |E_{\text{cal}}^*(A_{\text{res}}) - E_{\text{fus}}^*|$. Figure 5(a) displays the resulting estimated oxygen isotopic distribution. This distribution is wider with respect to model predictions and, more importantly, we find in the data a global shift toward neutron-poor isotopes, coherent with the finding of an extra experimental cross section for the $(xn, 2\alpha, {}^{16-x}\text{O})$ channel. Finally, it is important to stress that, with the exception of the anomalous branching ratio toward this channel, the detected events where the dissipated energy overcomes the four-body threshold associated with ${}^{15}\text{O}$ formation ($Q_{\text{kin}} = -15.78$ MeV) are fully compatible with a complete fusion pattern followed by the compound nucleus decay of ${}^{24}\text{Mg}^*$. Indeed, the HF calculation satisfactorily reproduces all the different observables that can be constructed with the exclusion of $Q_{>}$ events from the analysis and that do not directly involve α -oxygen coincidences. Figure 5 displays some selected examples, such as the velocity distributions of the heaviest fragment and the charge distribution of reaction products, this latter both for complete ($Z_{\text{det}} = 12$) and almost-complete ($Z_{\text{det}} \geq 10$) events, in order to show that no important bias is induced by the stringent completeness conditions. The global quality of the agreement between data and calculations indicates that our dataset corresponds to a component which is very close to the statistical decay of a hot equilibrated source, corresponding to the fused ${}^{24}\text{Mg}^*$ source. The only deviation with respect to the statistical model is therefore the extra α production in the oxygen channel.

IV. CONCLUSIONS

In conclusion, in this paper we have presented an exclusive analysis of dissipative ${}^{12}\text{C} + {}^{12}\text{C}$ collisions at 95 MeV, fully reconstructed in charge. A detailed comparison to a dedicated HF calculation shows an abnormally high branching ratio toward the $(2\alpha, {}^{16}\text{O}^*)$ channel with respect to the statistical expectation, where the oxygen is excited above its neutron emission threshold, which corresponds in part to the population of a doorway (${}^8\text{Be}-{}^{16}\text{O}^*$) configuration. This extra yield could be due to a failure of the HF theory for the decay of highly excited ${}^{24}\text{Mg}$, possibly due to the α correlations of this nucleus, which are already suspected to lead to specific high-lying (${}^{16}\text{O}-2\alpha$) resonances [16]. Alternatively, the compound nucleus hypothesis of full decoupling between entrance and exit channels could be questioned due to α correlations in the ${}^{12}\text{C} + {}^{12}\text{C}$ entrance channel. These two hypotheses cannot be discriminated by means of the present experimental information, but new data on ${}^{14}\text{N} + {}^{10}\text{B}$ at 80 MeV are currently under analysis.

ACKNOWLEDGMENTS

The authors thank the crew of the XTU TANDEM acceleration system at LNL. This work was partially supported by the European Funds for Large Scale Facilities, Seventh Framework Program, ENSAR 262010.

-
- [1] K. Ikeda, N. Takigawa, and H. Horiuchi, *Prog. Theor. Phys. Supplement* **E68**, 464 (1968).
- [2] M. Freer, *Rep. Prog. Phys.* **70**, 2149 (2007).
- [3] R. B. Wiringa, S. C. Pieper, J. Carlson, and V. R. Pandharipande, *Phys. Rev. C* **62**, 014001 (2000); Y. Kanada-En'yo and H. Horiuchi, *Prog. Theor. Phys. Supplement* **142**, 205 (2001); T. Neff and H. Feldmeier, *Nucl. Phys. A* **738**, 357 (2004).
- [4] E. Costanzo *et al.*, *Phys. Rev. C* **44**, 111 (1991); F. Grenier *et al.*, *Nucl. Phys. A* **811** 233 (2008); A. R. Raduta *et al.*, *Phys. Lett. B* **705**, 65 (2011); Tz. Kokalova, N. Itagaki, W. von Oertzen, and C. Wheldon, *ibid.* **96**, 192502 (2006); W. von Oertzen *et al.*, *Eur. Phys. J. A* **36**, 279 (2008); A. Di Pietro *et al.*, *J. Phys.: Conf. Ser.* **366**, 012013 (2012).
- [5] E. R. Cosman *et al.*, *Phys. Rev. Lett.* **35**, 265 (1975); C. A. Bremner *et al.*, *Phys. Rev. C* **66**, 034605 (2002); T. M. Cormier, C. M. Jachcinski, G. M. Berkowitz, P. Braun-Munzinger, P. M. Cormier, M. Gai, J. W. Harris, J. Barrette, and H. E. Wegner, *Phys. Rev. Lett.* **40**, 924 (1978); A. Morsad, F. Haas, C. Beck, and R. M. Freeman, *Z. Phys. A* **338**, 61 (1991).
- [6] A. H. Wuosmaa *et al.*, *Phys. Rev. Lett.* **68**, 1295 (1992); M. Aliotta *et al.*, *Z. Phys. A* **353**, 43 (1995); R. A. Le Marechal *et al.*, *Phys. Rev. C* **55**, 1881 (1997).
- [7] M. Takashina *et al.*, *Nucl. Phys. A* **738**, 352 (2004).
- [8] G. Baiocco, Ph.D. thesis, Università di Bologna and Université de Caen Basse-Normandie, 2012, <http://amsdottorato.cib.unibo.it/4295/>.
- [9] F. Gramegna *et al.*, *Nucl. Instrum. Methods A* **389**, 474 (1997); *Nuclear Science Symposium Conference Record*, 2004 IEEE **2**, 1132 (2004); A. Moroni *et al.*, *Nucl. Instrum. Methods A* **556**, 516 (2006).
- [10] M. D'Agostino *et al.*, *Nucl. Phys. A* **861**, 47 (2011); **875**, 139 (2012).
- [11] L. Morelli *et al.*, *Nucl. Instrum Methods A* **620**, 305 (2010).
- [12] The energy thresholds were 2, 6, 14, 20, 8 MeV, respectively, for p , d , t , ${}^3\text{He}$, and α particles. ${}^3\text{He}$ can be discriminated from α 's starting from 20 MeV. ${}^3\text{He}$ is estimated to represent less than 2%–3% of $Z = 2$ particles.
- [13] M. F. Rivet (INDRA Collaboration) and E. De Filippo (CHIMERA Collaboration) (private communications).
- [14] O. B. Tarasov and D. Bazin, *Nucl. Instrum. Methods B* **204**, 174 (2003).
- [15] R. J. Charity, *Phys. Rev. C* **82**, 014610 (2010).
- [16] T. Ichikawa, N. Itagaki, T. Kawabata, Tz. Kokalova, and W. von Oertzen, *Phys. Rev. C* **83**, 061301 (2011).